

# UCLA

## UCLA Previously Published Works

### Title

Quantitative multiparametric MRI in uveal melanoma: increased tumor permeability may predict monosomy 3.

### Permalink

<https://escholarship.org/uc/item/1xb4q3z5>

### Journal

Neuroradiology, 57(8)

### ISSN

0028-3940

### Authors

Kamrava, Mitchell  
Sepahdari, Ali R  
Leu, Kevin  
[et al.](#)

### Publication Date

2015-08-01

### DOI

10.1007/s00234-015-1546-0

Peer reviewed

# Quantitative multiparametric MRI in uveal melanoma: increased tumor permeability may predict monosomy 3

Mitchell Kamrava<sup>1</sup> · Ali R Sepahdari<sup>2</sup> · Kevin Leu<sup>2</sup> · Pin-Chieh Wang<sup>1</sup> · Kristofer Roberts<sup>1</sup> · D. Jeffrey Demanes<sup>1</sup> · Tara McCannel<sup>3</sup> · Benjamin M. Ellingson<sup>2</sup>

Received: 26 January 2015 / Accepted: 19 May 2015  
© Springer-Verlag Berlin Heidelberg 2015

## Abstract

**Introduction** Uveal melanoma is a rare intraocular tumor with heterogeneous biological behavior, and additional noninvasive markers that may predict outcome are needed. Diffusion- and perfusion-weighted imaging may prove useful but have previously been limited in their ability to evaluate ocular tumors. Our purpose was to show the feasibility and potential value of a multiparametric (mp-) MRI protocol employing state of the art diffusion- and perfusion-weighted imaging techniques.

**Methods** Sixteen patients with uveal melanoma were imaged with mp-MRI. Multishot readout-segmented echoplanar diffusion-weighted imaging, quantitative dynamic contrast-enhanced (DCE) MR perfusion imaging, and anatomic sequences were obtained. Regions of interest (ROIs) were drawn around tumors for calculation of apparent diffusion coefficient (ADC) and perfusion metrics ( $K^{trans}$ ,  $v_e$ ,  $k_{ep}$ , and  $v_p$ ). A generalized linear fit model was used to compare various MRI values with the American Joint Commission on Cancer (AJCC) tumor group and monosomy 3 status with significance set at  $P < 0.05$ .

**Results** mp-MRI was performed successfully in all cases. MRI tumor height (mean [standard deviation]) was 6.5 mm (3.0). ROI volume was 278 mm<sup>3</sup> (222). ADC was 1.07 (0.27) × 10<sup>-3</sup> mm<sup>2</sup>/s. DCE metrics were  $K^{trans}$  0.085/min (0.063),  $v_e$  0.060 (0.052),  $k_{ep}$  1.20/min (0.32), and  $v_p$  1.48 % (0.82). Patients with >33 % monosomy 3 had higher  $K^{trans}$  and higher  $v_e$  values than those with disomy 3 or ≤33 % monosomy ( $P < 0.01$ ). There were no significant differences between ADC ( $P = 0.07$ ),  $k_{ep}$  ( $P = 0.37$ ), and  $v_p$  with respect to monosomy 3.

**Conclusion** mp-MRI for ocular tumor imaging using multishot EPI DWI and quantitative DCE perfusion is technically feasible. mp-MRI may help predict monosomy 3 in uveal melanoma.

**Keywords** Uveal melanoma · Multiparametric MRI · Diffusion-weighted imaging · MR perfusion imaging · Personalized medicine

## List of abbreviations

DWI Diffusion-weighted imaging  
DCE Dynamic contrast-enhanced  
ADC Apparent diffusion coefficient  
CISS Constructive interference in steady state  
EPI Echoplanar imaging

## Introduction

Uveal melanoma is a rare tumor, with an annual incidence of approximately six per million and overall 5-year mortality reported at 16–53 %. It is both biologically and spatially heterogeneous

Mitchell Kamrava and Ali R Sepahdari contributed equally to this work.

✉ Ali R Sepahdari  
ali.sepahdari@gmail.com

<sup>1</sup> Department of Radiation Oncology, University of California Los Angeles, 200 Medical Plaza, Ste B265, Los Angeles, CA 90095, USA

<sup>2</sup> Department of Radiological Sciences, University of California Los Angeles, Los Angeles, CA, USA

<sup>3</sup> Department of Ophthalmology, University of California Los Angeles, Los Angeles, CA, USA

[1]. Though fine-needle aspiration biopsy can be used to identify prognostic markers such as monosomy 3 [2], noninvasive markers to stratify risk for metastasis are lacking.

To date, magnetic resonance imaging (MRI) of uveal melanoma has mostly been limited to describing features such as T2 signal, T1 signal, and contrast enhancement. Perfusion-weighted MRI of uveal melanoma has focused on describing the shape of the time-intensity curve; previously described techniques have lacked sufficient temporal resolution to determine quantitative pharmacokinetic information [3]. Diffusion-weighted imaging (DWI) of uveal melanoma has been performed [4, 5] but has only been used to distinguish uveal melanoma from surrounding retinal detachment, rather than to further characterize the biology of the tumor. DWI has notably been limited by magnetic susceptibility artifacts, precluding characterization of small tumors and degrading image quality overall [5]. Ideally, advanced MRI including DWI and perfusion-weighted imaging may be used to subcategorize uveal melanoma tumors by providing quantitative information for multiple vascular parameters, including permeability, washout rate, and interstitial space per unit volume, as well as estimates of the apparent diffusion coefficient (ADC), which is a surrogate marker for cellularity. Correlating the diffusion and perfusion characteristics with known prognostic markers, such as monosomy 3, may ultimately expand the role of advanced imaging in uveal melanoma from diagnostic to prognostic.

The purpose of this study is to show the feasibility of a multiparametric MRI protocol for ocular melanoma imaging, using quantitative dynamic contrast-enhanced (DCE) MR-perfusion imaging employing echoplanar imaging (EPI) T1-weighted imaging and DWI using a multishot EPI sequence that reduces susceptibility artifact. A subsequent exploratory analysis of mp-MRI characteristics with monosomy 3 status was also evaluated.

## Methods

### Subjects

This Health Insurance Portability and Accountability Act complaint, Institutional-Review-Board-approved study was performed with a waiver of informed consent. Consecutive patients imaged with a multiparametric ocular tumor MRI protocol were prospectively studied. Sixteen subjects, 5 female and 11 male, with primary uveal melanoma were imaged over a 33-month period. The subjects had an average age of 59 years (range 27–77).

### MRI

Detailed parameters of each sequence can be found in Table 1. A 1.5-T MR scanner was used for all image acquisition

(Avanto; Siemens Healthcare AG, Erlangen, Germany). Patients were instructed not to wear eye makeup and to keep their eyes closed during scanning. Pre-contrast sagittal and axial T1-weighted spin-echo, axial heavily T2-weighted three-dimensional constructive interference in the steady state (CISS) sequences, and axial multishot EPI DWI were obtained through the orbits. The CISS images were reformatted in oblique planes in order to obtain tumor measurements. DWI was performed with a multishot (nine shots), spin-echo, EPI sequence with  $b=0$  and  $800 \text{ s/mm}^2$  (RESOLVE). An ADC map was generated from the  $b=0$  and  $800 \text{ s/mm}^2$  data sets. Tumors were manually contoured on the ADC maps on multiple slices using the OsiriX viewer for Mac [6], and an average ADC was obtained for each tumor based on the contoured volume. Following DCE-MRI acquisition (below), a post-contrast axial T1-weighted spin-echo sequence was obtained.

### DCE-MRI

Initially, fast low-angle shot (FLASH) images with flip angles of  $2^\circ$ ,  $5^\circ$ ,  $15^\circ$ ,  $20^\circ$ , and  $25^\circ$  were acquired in four matched slices through the center of the tumor. Dynamic FLASH images with a flip angle of  $25^\circ$  were then acquired at a 6-s temporal frame rate during a  $5 \text{ cm}^3/\text{s}$  bolus injection of  $0.1 \text{ mmol/kg}$  Gd-diethylene triamine pentaacetic acid (DTPA), followed by a 20-cc injection of isotonic saline, with a 30-s baseline. Seventy time points were obtained over the 7-min acquisition time.

DCE-MRI post-processing consisted of first using the Ernst angle [4] equation to fit T1 to the multiple flip angle data on a voxel-wise basis using the nonlinear least squares regression algorithm (*3dNLFit*) in AFNI (*Analysis of Functional Neuroimages Software Package*; NIH/NIMH; <http://afni.nimh.nih.gov/afni>), using in-house MATLAB scripts. The DCE-MRI dynamic time series was then converted to a dynamic series reflecting the change in T1 with respect to the established baseline ( $\Delta R1(t)$ ). A dynamic concentration versus time series ( $C(t)$ ) was then created from the dynamic T1 time series, assuming a relaxivity of Gd-DTPA of  $4.5/\text{mM s}$  [7]. All DCE-MRI images for each subject and scan session were registered to the baseline T1-weighted post-contrast image using a 12-degree-of-freedom affine transformation and a mutual information cost function to account for motion between each image sequence (FMRIB Software Library (FSL); FMRIB, Oxford, UK; <http://www.fmrib.ox.ac.uk/fsl/>). If required, manual alignment was subsequently performed (tkregister2, Freesurfer; [surfer.nmr.mgh.harvard.edu](http://surfer.nmr.mgh.harvard.edu); Massachusetts General Hospital, Harvard Medical School).

Manual regions of interest (ROIs) were drawn within both internal carotid arteries (ICAs), which were used as the

**Table 1** Detailed MRI pulse sequence information

	Axial T1 (pre- and post-contrast)	Sagittal T1	Axial 3D-CISS	Multishot DWI (RESOLVE)	DCE-MRI <sup>a</sup>
TR/TE (ms)	400/7.8	400/7.8	5.42/2.42	2500/72	27/2.87
FOV (mm)	157×160	230×130	135×180	229×229	119×239
Matrix	256×214	320×224	256×192	224×224	448×202
Slick thickness/gap (mm)	3/0	5/1.5	0.7/0	2.5/0	3/0
Flip angle	90	90	70	90	25
NEX	2	1	1	3	1

TR repetition time, TE echo time, FOV field of view, NEX number of excitations, CISS constructive interference in steady state, DCE dynamic contrast-enhanced

<sup>a</sup> DCE-MRI was performed with parallel acceleration factor of 2 and 6/8 partial Fourier acquisition

patient-specific arterial input function (AIF) as previously described [8]. Nonlinear least squares regression was used to fit the dynamic concentration versus time curves  $C(t)$  to the standard three-parameter Tofts model [9, 10], on a voxel-by-voxel basis to extract parameters of interest:  $K^{trans}$  (vascular permeability in /min),  $v_e$  (interstitial space per unit volume of tissue [unitless]),  $k_{ep}$  (flux rate constant between the extravascular and extracellular space and blood plasma), and  $v_p$  (fractional plasma volume). Voxels with a significant fit to model parameters (i.e.,  $r^2 > 0.7$  and a level of significance  $P < 0.05$ ) were retained for analysis. ROIs were then defined on post-contrast, T1-weighted images for the region of contrast-enhancing solid tumor and normal-appearing white matter (NAWM) in the pons (Fig. 1).

## Treatments

Patients underwent intraoperative transscleral fine-needle biopsy aspiration during plaque brachytherapy. Biopsy specimens were processed for cytopathologic and cytogenetic analysis. Chromosome 3 status was evaluated at the University of California Los Angeles Clinical Cytogenetics Laboratory, a standardized CLIA-approved laboratory with a cytogeneticist experienced in interpreting and reporting fluorescent in situ hybridization (FISH) results for uveal melanoma. Cells collected for cytogenetic analysis were gently spun down in a sterile conical tube and resuspended in Roswell Park Memorial Institute 1640 (RPMI-1640) media (Gibco [Invitrogen], Carlsbad, CA, USA) supplemented with antibiotics and 10 % bovine serum (Irvine Scientific, Santa Ana, CA, USA). The cultures were prepared according to standard protocols. For FISH analysis, a directly labeled centromeric probe specific for chromosome 3, CEP-3 Spectrum Orange (Vysis, Downers Grove, IL, USA), was used to assess monosomy or disomy. This probe was hybridized to fixed cultured cells following the manufacturer's protocol (Abbott-Vysis, Des Plaines, IL, USA). Hybridization signals were counted

by hand in nonoverlapping nuclei of cells under a fluorescence microscope (Axiophot, Carl Zeiss Mikroskopie, Jena, Germany) equipped with a triple filter (diamino-2-phenylindole dihydrochloride/fluorescein isothiocyanate/Texas Red). When any cells were found to contain only one copy of chromosome 3, the sample was considered positive for monosomy 3.

## Statistical analysis

A generalized linear fit model was used to compare various MRI values with the American Joint Commission on Cancer (AJCC) tumor group and monosomy 3 status. In the analysis of monosomy 3 status, a cutoff of 33 % was employed based on published data demonstrating its significance in metastasis-free survival [2].  $P < 0.05$  was considered significant.

## Results

A total of 16 patients with primary uveal melanoma underwent mp-MR (Table 2, online only). The average  $\pm$  standard deviation (SD) MRI tumor height was  $6.5 \pm 3.0$  mm. ROIs were identified and contoured for each patient with the average  $\pm$  SD volume being  $278 \pm 222$  mm<sup>3</sup>. Mean  $\pm$  SD ADC for all patients was  $1.13 \pm 0.36 \times 10^{-3}$  mm<sup>2</sup>/s. The mean  $\pm$  SD DCE metrics of  $K^{trans}$ ,  $v_e$ ,  $k_{ep}$ , and  $v_p$  were  $0.085 \pm 0.063$ /min,  $0.060 \pm 0.052$ ,  $1.20 \pm 0.32$ /min, and  $1.48 \pm 0.82$  %, respectively (Table 3, online only). NAWM was used as an internal control to help confirm measurement validity.  $K^{trans}$  value for NAWM was consistent with published values [11].

A comparison of AJCC stage and the mp-MRI parameters ADC,  $K^{trans}$ ,  $v_e$ ,  $k_{ep}$ , and  $v_p$  was performed to investigate any correlations. The distribution of AJCC groups 1, 2, 3, and 4 was three, six, six, and one patients, respectively. There were no significant correlations between mp-MRI parameters and AJCC group.

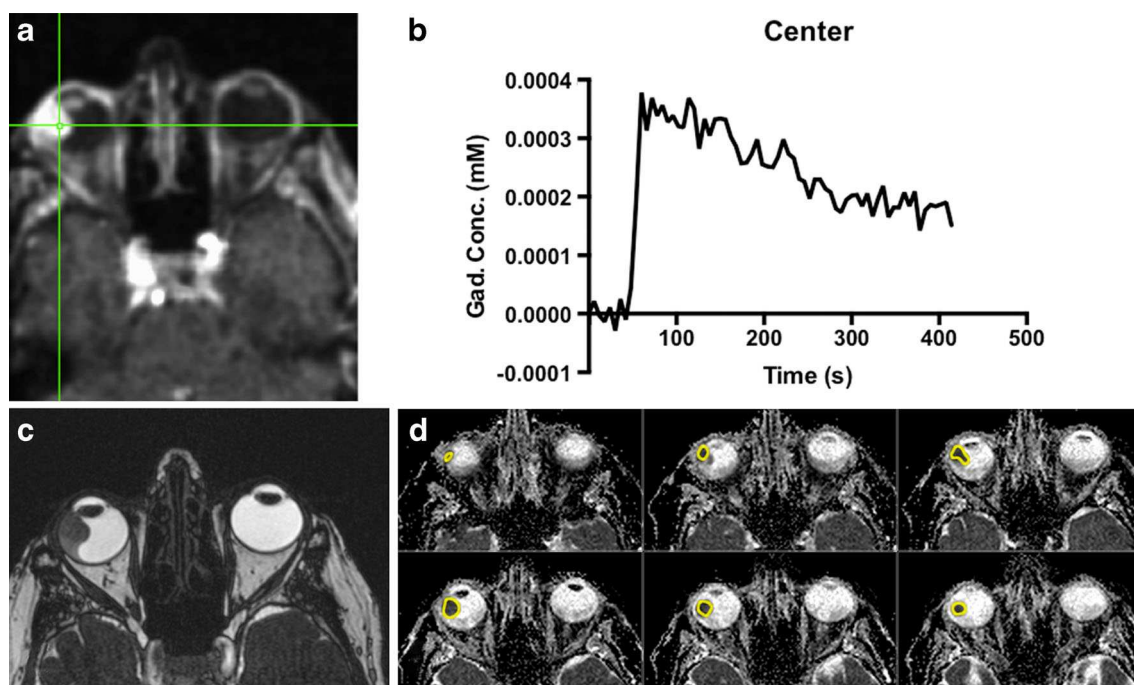


**Fig. 1** Representative example of multiparametric MRI. Right ocular melanoma, exhibiting monosomy 3. **a** Average intensity projection image from dynamic MR perfusion time series, with a sample voxel placement (note that the entire lesion was contoured for data analysis). **b** Time-intensity curve from the voxel sampled in **a** shows rapid wash-in of contrast, consistent with elevated  $K^{trans}$ . **c** Axial constructive interference in the steady-state MR image shows sharp demarcation

between hypointense tumor anteriorly, hyperintense vitreous humor, and intermediate signal fluid beneath a detached retina. These images were reformatted in oblique planes to obtain tumor measurements. **d** Axial apparent diffusion coefficient images from multishot EPI diffusion-weighted imaging visualize the tumor well, without anatomic distortions. The tumor is readily contoured on multiple contiguous slices

Signal-to-noise ratio (SNR) measurements were obtained from six representative AJCC group 1, 2, and 3 tumors. SNR

**Table 2** Patient characteristics

Patient no.	Age at diagnosis (years)	MRI tumor height (mm)	MRI basal dimensions (mm)
1	66	9	8.9×8.5
2	72	2	15×8
3	68	2	6.5×6.5
4	74	2	6.1×7.0
5	57	8	15.1×12.8
6	77	7.5	8.3×9.3
7	43	7	8.2×9.1
8	51	9.5	15.5×11.9
9	37	9	12.8×11.1
10	73	4.5	12.3×11.9
11	57	4.7	15.7×14.3
12	58	3.5	9×9
13	67	11	14×11
14	54	9	15×18
15	57	7.6	20.2×19.7
16	61	8.1	15.4×17.5

was calculated as the mean of the tumor at baseline minus the mean of the background divided by the standard deviation of the baseline.

The AJCC group 1 tumors had a mean SNR of 4.4. Group 2 tumors had a mean SNR of 5.0. Group 3 tumors had a mean SNR of 7.5. Lower SNR in small tumors was reflected in visual analysis of the time-intensity curves (TICs), which showed wider point-to-point variations compared to TICs of larger tumors (Fig. 2).

Tumors were evaluated with fine-needle aspiration performed at the time of plaque placement. Fine-needle aspiration was performed in all patients, but sufficient material for diagnosis was obtained in only 12 of 16 cases. Of these, 7/12 did not have monosomy 3, 4/12 had monosomy 3 in >33 % of the examined cells, and 1/12 had monosomy 3 in ≤33 % of the examined cells. There was a significant correlation between  $K^{trans}$  and monosomy 3 >33 % (Fig. 3) and between  $v_e$  and monosomy 3 >33 % ( $P<0.01$ ). Patients with >33 % monosomy 3 had higher  $K^{trans}$  than those with disomy 3 or ≤33 % monosomy 3 (0.145 versus 0.061/min,  $P<0.01$ ). No significant differences were found between  $k_{ep}$  ( $P=0.37$ ) values and monosomy 3 status. There was a nonsignificant trend toward lower ADC in monosomy 3 ( $0.80±0.07$ ) than in disomy 3 or ≤33 % monosomy 3 ( $1.03±0.20$ ), with  $P=0.07$ . There was also a nonsignificant trend toward higher  $v_p$  in monosomy 3

